Effect of aging on the magnetic characteristics of nickel nanowires embedded in polycarbonate

K. Maaz,[1,2] S. Ishrat,[1] S. Karim,[2] and Gil-Ho Kim[1,a)]
[1]*Department of Electronics and Electrical Engineering and Sungkyunkwan University Advanced Institute of Nanotechnology (SAINT), Sungkyunkwan University, Suwon 440-746, Korea*
[2]*Nanomaterials Research Group, Physics Division, PINSTECH, Nilore, Islamabad, Pakistan*

(Received 15 January 2011; accepted 22 May 2011; published online 6 July 2011)

Single crystalline Ni nanowires (with a controlled diameter of ~14 nm) have been fabricated by electrochemical deposition in etched ion-track polycarbonate templates. The exchange bias effect in these nanowires has been studied at 10 K under a cooling field of 10 kOe applied parallel to the wire axis for different time intervals starting from the as-fabricated to ~2 yr old samples. A continuous drop in the saturation magnetization has been observed with time due the formation of an antiferromagnetic oxide layer at the periphery of nanowires. A model for the drop of magnetization has been used to calculate the thickness of the oxide layer in nickel nanowires. The observed variation in exchange bias and saturation magnetization has been explained by taking into account the exchange interactions at the Ni-NiO interface and the development of antiferromagnetic NiO at the expense of metallic Ni. © *2011 American Institute of Physics*. [doi:10.1063/1.3603006]

INTRODUCTION

One-dimensional nanostructures like nanowires (NWs), nanotubes, and nanobelts, are currently the subject of immense interest because of their potential applications in the electronics, computer, recording, biological, and medical industries.[1,2] In particular, transition metal oxide nanostructures are important for data storage and spin-valve devices as the magnetic materials.[3] The magnetic properties of nanomaterials are usually different from their bulk counterparts because of their high surface to volume ratio of spins that cause finite size effects in these materials. In the nanoscale regime, where one or more dimensions are reduced to the order of the domain wall length or the exchange length, the magnetic properties become strongly dependent on the structural geometry of the materials. It is now well-established that in nanostructured materials, the surface spins play a crucial role as far as their magnetic properties are concerned. These spins cause, for example, a reduction in the saturation magnetization and the enhancement of coercivity, or the appearance of exchange bias at lower temperatures. In these materials the surface spins do not follow the core anisotropy-direction and become disordered or canted, leading to the formation of a magnetic bilayer system with different magnetic orders. In the case of nickel nanowires, the outer layer is generally NiO, which is magnetically antiferromagnetic (AFM), while the inner layer is Ni which is ferromagnetic (FM). The formation of the AFM (NiO) layer is basically at the expense of the metallic FM (Ni) and therefore is associated with a general loss of magnetization in these nanowires.

Temperature dependent magnetic analyses in multilayer systems lead to several interesting phenomena, including the exchange bias (H_{EB}) effect.[3,4] The exchange coupling at the FM-AFM interface may induce unidirectional anisotropy in FM materials, below the Néel temperature of the AFM, shifting the loop along the field axis.[4] The exchange bias effect, H_{EB}, has also been observed in other bilayer systems involving ferromagnetic, ferrimagnetic, and spin-glass-like materials.[3,4] This phenomenon has mainly been investigated in thin films and to some extent in nanoparticles.[5–7] However, this effect has been recently observed in 1-dimensional (1-D) nanostructures as well.[8,9] In 1-D nanostructures (e.g., nanowires), well-defined hard and easy axis exists due to the strong shape anisotropy, especially in cylindrical nanowires that plays a crucial role in determining both the magnitude and the direction of H_{EB} in such systems. The competition between the shape and field-cooled induced anisotropies can be tailored to study the magnetic properties and exchange bias effect in multilayered nanowires.

In template embedded NWs, the H_{EB} can be used as a tool for investigating the oxidation rate at the surface of the NWs. The polymer hosting nanowires provide protection against rapid oxidation, thereby slowing down the oxidation rate in the wires. The thickness of the oxide layer depends on the nature of the polymer-wire interface; because the (polycarbonate) PC protects the NWs against their rapid oxidation although it is permeable to the atmospheric oxygen.[10] In the case of Co NWs ~30 nm in diameter embedded in PC an average oxide layer of ~4 nm in thickness has been measured after a delay time 800 days from the sample's fabrication.[11] While in the case of Co thin films (> 5 nm), a layer of ~2.5 nm thickness has been reported within the initial first few days of their fabrication.[12] In both cases, it has been observed that the oxidation rate is high at the start and the thickness of the oxide layer increases monotonically with time, while a steady state oxidation is achieved afterwards. Soon after the fabrication of the NWs there is no evidence of

a)Author to whom correspondence should be addressed. Electronic mail: ghkim@skku.edu.

H_{EB} due to the absence of the AFM oxide layer at the periphery of the wires. However, after a few days, a significant contribution to the H_{EB} arises as a result of the formation of the AFM layer at the surface of the wires exposed to the atmospheric conditions. The oxidation of the NWs, in general, causes a loss in their magnetization as a result of the development of the AFM oxide layer at the expense of the FM metallic layer.

In this article we present the fabrication of single crystalline Ni NWs by electrochemical deposition in ion track-etched polycarbonate (PC) templates. At various stages, oxide layer thicknesses have been calculated from the experimental values of the magnetization drop and the results have been verified by transmission electron microscopy and x-ray diffraction techniques.

EXPERIMENTAL PROCEDURES

Polycarbonate foils 30 μm in thickness were irradiated at normal incidence with ^{238}U ions (kinetic energy: 11.4 MeV/u, fluence: 10^8 ions cm^{-2}). Each ion creates a cylindrical damage zone along its trajectory which was further sensitized by UV light irradiation for 2 h. The UV irradiation enhanced the track-etching rate, thus supporting the formation of cylindrical tracks in the PC membranes.[13,14] The foils were subsequently etched in 5 M NaOH solution at 50 °C to obtain the cylindrical nanopores. The diameter of the etched pores was controlled by the etching-time during the process of etching. In the next step, a thin gold layer ($\sim$10 nm) was sputtered onto one side of the membrane and subsequently reinforced by an electrochemically deposited copper layer of $\sim$5 μm. This layer served as a cathode during the wires fabrication process, while a metallic nickel rod was used as the anode. The electrolyte consists of 1 M $NiSO_4$ and the initial *p*H of the solution was adjusted to 6 by adding the appropriate amount of H_2SO_4. The deposition of Ni was carried out using a constant voltage of -0.95 V at room temperature; further details are given in Ref. 15. The morphology of the NWs was investigated by scanning electron microscopy (SEM) and high-resolution transmission electron microscopy (TEM), while the composition of the wires was studied by means of energy dispersive spectroscopy (EDS). The x-ray diffraction (XRD) technique was used for analyzing the texture of the nanowires. Additionally, magnetic characterization has been performed by a quantum design physical property measurement system up to a maximum field of 20 kOe. For SEM and TEM analyses, the nanowires were liberated from the template by dissolving the PC in dichloromethane (CH_2Cl_2). For magnetic and XRD characterizations the wires were left embedded in the template and the Au/Cu substrate layer was removed.

RESULTS AND DISCUSSION

Figures 1(a) and 1(b) show the SEM images of the as-prepared Ni nanowires liberated from the PC templates. Figure 1(a) shows the lateral view of the Ni NWs representing $\sim$24 μm length of the wires, while Fig. 1(b) shows the vertical view of the wires. In Fig. 1(b) the NWs are standing vertically, mostly in the form of bundles. Possible reasons for

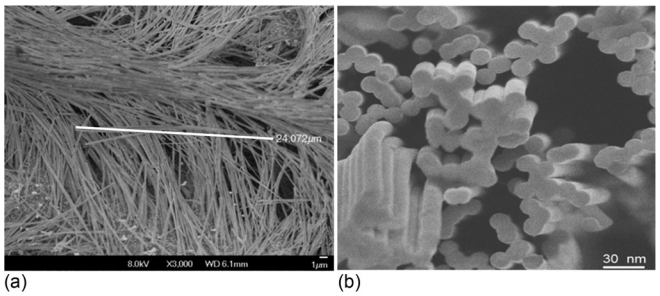

FIG. 1. SEM image of (a) horizontal view of Ni NWs lying on the substrate along the direction of the dissolving liquid, indicating the length of the wires. A maximum length of $\sim$24 μm can be seen in the images, and (b) the vertical view of the NWs in the form of bunches of wires. These are formed due to their magnetic nature and high aspect ratio.

the bundle formation are: (1) the magnetic force in the Ni NWs that keeps them together in the form of bundles, and (2) the aspect ratio ($l/d \approx 2100$) of the wires is very high, therefore it is difficult for an individual NW to stand without any support. In the SEM images the NWs are observed to be cylindrical in shape with homogenous contours over their whole length. Due to the good quality of the polymeric templates used in this work the diameter distribution within a given sample was $\sim$7% of their mean value. In this work, homemade PC membranes were used rather than commercially purchased ones. The shape of the pores in commercially available membranes is usually toothpick- or cigar-like.[16,17] In such membranes the wires that are grown are generally wider in the centers and thinner at the ends.[16] Figure 2 shows the high resolution TEM image of the as-prepared Ni NWs with a mean diameter of $\sim$14 nm. The inset of the figure shows the selected-area electron diffraction (SAED) pattern of a randomly selected segment of a wire. The SAED analysis shows that the as-prepared Ni NWs are

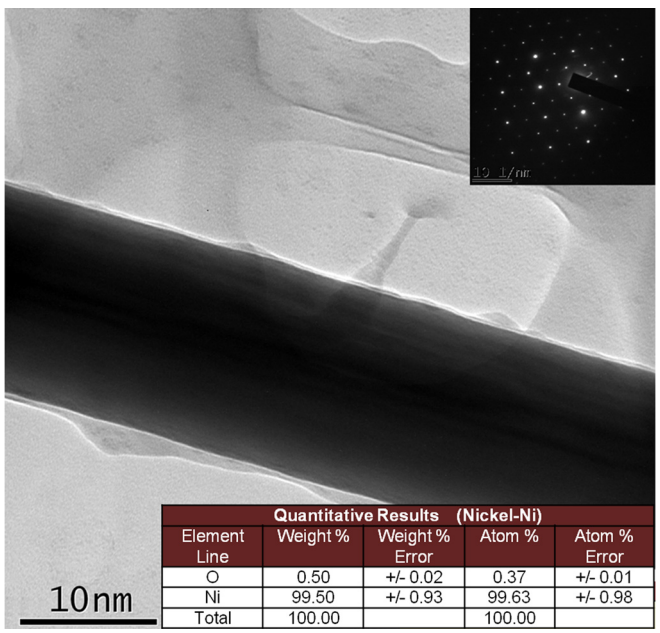

FIG. 2. (Color online) TEM micrograph of single-crystalline Ni nanowires with a diameter of $\sim$14 nm. The inset figure shows the SAED analysis of one of the wires while the inset table shows the EDS results of a segment of the same wire.

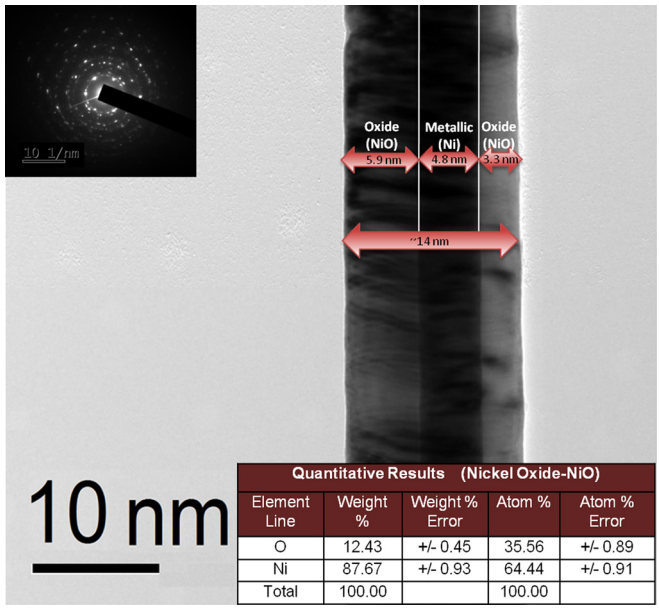

Quantitative Results (Nickel Oxide-NiO)				
Element Line	Weight %	Weight % Error	Atom %	Atom % Error
O	12.43	+/- 0.45	35.56	+/- 0.89
Ni	87.67	+/- 0.93	64.44	+/- 0.91
Total	100.00		100.00	

FIG. 3. (Color online) TEM micrograph of ~2 yr old Ni nanowires representing metallic Ni at the center surrounded by the thick NiO layer. The inset figure and table show the corresponding SAED and EDS results of a single nanowire.

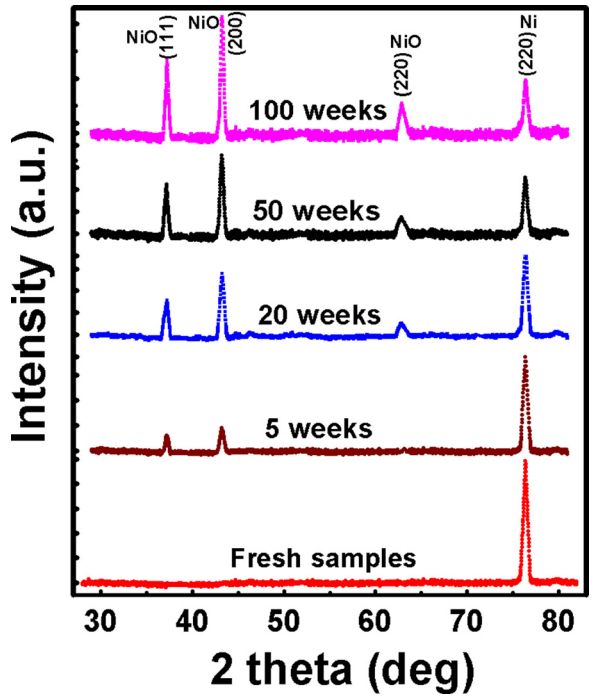

FIG. 4. (Color online) XRD patterns of Ni NWs at different stages starting from the as-prepared to 100 week old samples. The change in intensity of the Ni and NiO peaks represents the time varying transformation of Ni into NiO.

single crystalline with face centered cubic (fcc) structure. Moreover, the EDS results shown in the inset table of Fig. 2 reveal that the prepared sample is composed of purely metallic Ni with no evidence of any oxidation in the form of NiO. Figure 3 shows the TEM images of 100 week (~2 yr) old Ni NWs with SAED and EDS analyses of these samples shown in the inset of the figure. The TEM image in Fig. 3 shows that Ni NWs, after 2 yr, are now surrounded by a few nanometers thick layer of nickel oxide. This oxide layer is usually polycrystalline and sometimes multiphase as well.[18] The polycrystalline behavior of 2 yr old NWs is evident in the SAED image of the wires. The quantitative results of the EDS show that the NWs, after 2 yr, are now composed of metallic Ni along with its oxide (NiO) that arises from the oxidation of Ni in the presence of atmospheric oxygen. Additionally, the TEM images confirm the cylindrical morphology and uniform contour of the wires. In general, the TEM and SAED analyses of the as-prepared NWs show no grain boundaries, thus confirming that our Ni NWs consist of at least several micrometer long single-crystals. Figure 4 displays the XRD patterns of Ni NWs at five different stages starting from the as-prepared to 100 weeks older samples. All the reflections shown in the XRD patterns are indexed for Ni and NiO. In the as-prepared samples, only the Ni (220) reflection is present, which shows the single crystalline nature and strong 110 texture of the wires. After a waiting period of 5 weeks NiO reflections start to appear in the XRD pattern that can be indexed in accordance with JCPDS card No. 47-1049 for nickel oxide. The XRD patterns illustrate that the intensity of the NiO peaks increases with time as a result of the increasing thickness of the Ni-oxide layer with time at the preferential surface of the NWs. It is interesting to note that the intensity of the Ni (220) reflection diminishes with time because of the increasing oxidation of Ni and therefore the content of Ni decreases while NiO increases with time.

Magnetization curves of the embedded Ni nanowire arrays with the magnetic field applied parallel to the long wire axis at 10 K are shown in Figs. 5(a)–5(d). The insets of the figures show the expanded region around the origin for the visibility of the reader. Figure 5(a) shows the zero field cooled (ZFC) magnetization curve of the as-prepared Ni NWs with a maximum field up to 20 kOe. The single-crystalline NWs possess a coercivity of ~692 Oe at 10 K while at room temperature the coercivity is ~100 Oe indicating that the coercivity has been increased by a factor of ~7 at 10 K. This is well corroborated with the reported coercivity value of 101 Oe at 300 K for single crystalline nickel nanowires with diameters of ~50 nm.[19] The very large coercivity at low temperature is consistent with the pronounced growth of the magnetic anisotropy inhibiting the alignment of the moment along the applied field direction. Figures 5(b)–5(d) show the field cooled (FC = 10 kOe) magnetization curves of the Ni NWs aged 10, 50, and 100 weeks, respectively. In the case of the ZFC curve shown in Fig. 5(a), the loop is symmetric about the origin while in FC conditions; the loops show a horizontal shift along the field axis opposite to the direction of the cooling field. These features are the characteristics of exchange bias defined by $H_{EB} = (H_{c1} + H_{c2})/2$, where H_{c1} and H_{c2} are the left and right coercivities of the field cooled magnetization curve, respectively. The values of H_{EB} calculated from the FC curves are plotted as a function of the age of the Ni NWs and are shown in Fig. 6(a). It is seen that H_{EB} increases linearly, quite rapidly within the first 15–20 weeks, indicating a rapid oxidation of the wires in the initial weeks. In the subsequent time, the increase in H_{EB}

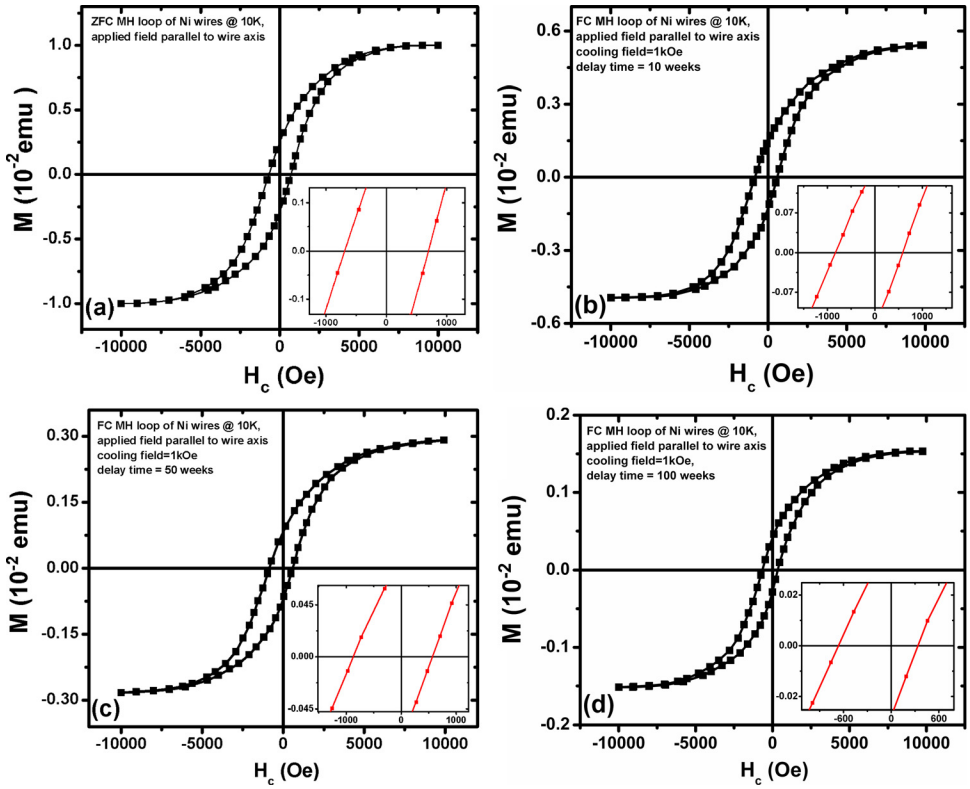

FIG. 5. (Color online) Magnetization hysteresis loops of Ni NWs embedded in PC templates. (a) Shows the ZFC hysteresis curve of 14 nm single crystalline NWs. (b)–(d) Show the FC hysteresis curves of the NWs aged 10, 50, and 100 weeks, respectively. The insets of the figure show the expanded region around the origin for the visibility of the reader.

becomes slower and almost constant, indicating a steady state oxidation for ~1 yand finally an increasing trend is observed in H_{EB} values NWs aged for ~2 yr. The absence of H_{EB} in fresh samples indicates that there is no AFM oxide layer at the surface of the NWs however, as time passes, because of the rapid growth of the oxide layer at the periphery of NWs, an exchange bias effect arises and plays a role. To explain various trends in H_{EB} versus the time curve it is assumed that in Ni NWs the AFM NiO is formed at the expense of the FM Ni and the thickness of this layer increases with time. Since there is fast oxidation of the wires in the initial weeks, H_{EB} increases rapidly with the NiO

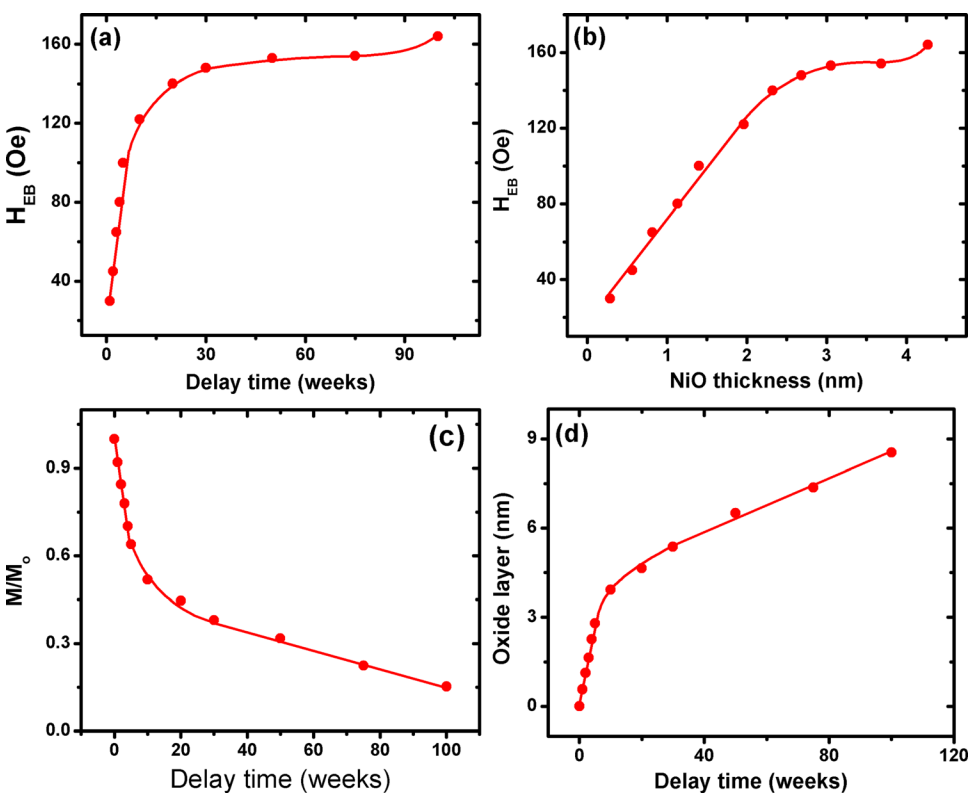

FIG. 6. (Color online) (a) Variation of H_{EB} as a function of the delay time after the wires have grown. The values have been calculated from FC magnetization curves of the samples for different delay time intervals. (b) H_{EB} as a function of the NiO layer thickness, (c) M/M_o as a function of delay time, and (d) NiO thickness as a function of the age of the wires.

thickness up to ~3 nm and then becomes nearly constant, as shown in Fig. 6(b). In fact, the dependence of H_{EB} on the AFM thickness is quite complicated. However, in the case of thin films, as the thickness of the AFM increases (above a few nm) H_{EB} increases rapidly and finally, for thick enough AFM layers (~tens of nm) H_{EB} becomes independent of the AFM thickness.[20] In our case, for the NiO layer thicker than 3 nm, there seems to be no substantial increase in H_{EB}, as shown in Fig. 6(b). This may be due to two reasons: (1) the microstructural changes in the AFM NiO with increasing thickness, e.g., one type of phase or orientation is no longer stable above certain thicknesses, and (2) changes in the AFM domain structure that may arise with the AFM layer thickness.[21] The microstructural changes in NiO will be the possible reason in our case. Now we will refer to Fig. 6(a), where there seems to be an increasing trend of H_{EB} after 80 weeks. A similar trend can be observed in Fig. 6(b). This increase in H_{EB} can be explored if we account for the FM layer thickness that plays a crucial role while studying the exchange bias effect in thin films or nanowires.[22] The dependence of H_{EB} on the FM layer thickness was explored in detail by Kung *et al.*[23] They studied a system composed of 3 interfaces of NiFe(60 nm)/FeMn(4–40 nm)/NiFe(30 nm)/Ta(20 nm). The H_{EB}, in terms of the interfacial energy density (S in erg/cm^2), magnetization (M), and FM layer thickness (t_{FM}), is defined by the relation, $H_{EB} = S/Mt_{FM}$. From this relation it is clear that H_{EB} is inversely related to both the thickness of the FM material and its magnetization. Now, if we analyze our data and consider that the preceding relation holds for our system of Ni NWs, then as the thickness of Ni, which converts to NiO with time, is going to decrease, H_{EB} increases. This conversion also decreases the effective magnetic volume and hence, the magnetization decreases which results in an increase in H_{EB}, according to the preceding relation. It is, therefore, expected that H_{EB} will be high after a long time (e.g., ~2 yr in our case). However, if the FM layer is too thin (e.g., after a very long time delay, all Ni is converted to NiO) then this relation may not hold further.[19,22,24] This is because for a thin enough layer the FM may become discontinuous. The thickness at which this occurs (usually a few nm) varies from system to system and depends on the microstructure and growth mechanisms of the FM materials.[19,25–27] It is interesting to note that the maximum value of the exchange bias after 100 weeks in our case is ~170 Oe. This value is, however, smaller than the exchange bias value of 220 Oe reported for Ni/NiO nanowires deposited onto the CNT/Pt nanocomposites.[28] The difference between the two values could be either the result of FM/AFM layer thicknesses or the operating temperatures, that are different in both cases. Another possibility of the smaller H_{EB} can be the smaller cooling field (1 kOe) used in our case, while in their case they have reported a cooling field of 5 kOe.

To carry out the quantitative analysis of the oxidation layer around the Ni NWs one can record the drop in normalized magnetization at saturation (M/M_o) as a function of time. The thickness of the oxide layer can be calculated at various oxidation states of Ni NWs using the experimental values of the magnetization drop given in Fig. 6(c). In fact, the magnetization is directly related to the oxide layer thickness and the remaining magnetic material (Ni). Figure 6(c) shows the normalized magnetization at saturation (M/M_o), where M_o is the value of the magnetization of fresh samples and M is the remaining magnetization. From this figure, it is seen that M/M_o shows a continuously decreasing behavior, which is sharp in the beginning and then becomes slower after ~20 weeks, similar to the behavior of H_{EB} with time. The rapid drop of the magnetization is, in fact, due to the rapid oxidation of the wires, where FM Ni is converted into AFM NiO as a result of the oxidation of the wires in the atmospheric oxygen. It is noticeable that the value of the magnetization of the NWs and the effective magnetic volume (V) are related to each other by the relation $M = M_sV$, where M_s is the saturation magnetization of bulk nickel. In this relation, the decrease in magnetization due to the top and bottom faces of NWs are neglected because the length (l) of the Ni nanowires is very long (~30μ) as compared to diameter (~14 nm) of the wires. Therefore, the contribution from the top and bottom surfaces toward the magnetization is negligible as compared to the preferential surface of the NWs. The normalized magnetization (M/M_o) can be approximated by the reduced magnetic mass (m/m_o) of Ni and thus to the ratio (R^2/R_o^2 using the mass-density relation). Where R is the radius of Ni with magnetic mass (m), and m_o and R_o are the mass and radius of the as-prepared Ni nanowires. The oxide layer thickness $\Delta R = R_o - R$ is given by $\Delta R \approx R_o[1 - (M/M_o)^{1/2}]$.[11] In the case of Ni NWs, the oxidation state of the wires for different delay times can be calculated from the values of M/M_o given in Fig. 6(c). The thickness of the oxide layer, as a function of the calculated delay time using the preceding equation, is given in Table I. It is seen that after ~2 yr delay time the total oxide layer is ~8.5 nm, which is in good agreement with the results of the TEM that is ~9 nm. From Fig. 6(c) it is seen that a larger drop in magnetization, about 50%, occurs in the initial few (~10) weeks, while only about 35% magnetization drop occurs in the remaining 90 weeks, indicating a rapid oxidation in the initial weeks.

TABLE I. NiO layer thickness (nm) calculated from normalized magnetization values for different delay times (weeks) for 14 nm Ni nanowires.

Delay time (weeks)	M/M_0	$\Delta R = R_0 - R$	NiO thickness (nm)
0 (fresh sample)	1	0	0
1	0.92	0.28	0.57
2	0.84	0.56	1.13
3	0.78	0.82	1.64
4	0.70	1.13	2.27
5	0.64	1.40	2.80
10	0.52	1.96	3.92
20	0.44	2.32	4.65
30	0.38	2.68	5.37
50	0.32	3.05	6.10
75	0.22	3.68	7.37
100	0.15	4.27	8.54

The larger magnetization drop in our case is in accordance with the prediction of a larger magnetization drop in smaller diameter NWs.[11] Figure 6(d) shows the thickness of the oxide layer as a function of the delay time where we can conclude similar results of rapid oxidation in the initial

weeks and a steady state oxidation in the subsequent weeks. Further oxidation at the interiors of the nanowires is expected to be slower because of the outer oxide layers that are protecting metallic Ni at the center from atmospheric oxygen, thereby slowing down the oxidation rate in Ni nanowires.

CONCLUSION

Magnetic NWs have been fabricated by electrochemical deposition in etched PC templates. Our SEM and TEM analyses confirm the cylindrical shape and uniform contour of the wires while the SAED and EDS results reveal that the as-prepared NWs are completely in single crystalline form while the aged NWs are in mixed form. Rapid oxidation has been found in the initial weeks while a steady state oxidation has been found after about 20 weeks in accordance with the fact that the outer layers prevent the rapid oxidation of Ni at the center of the NWs. Variation in the exchange bias with time showed a sharp increase in the beginning while showing a slower increase afterwards that has been attributed to the fast development of the AFM NiO layer at the start, which becomes slower after about 15–20 weeks. A continuous decrease in saturation magnetization has been recorded at the surface of the wires due to the natural oxidation of Ni into Ni-oxide. From the drop of the magnetization, the thickness of the oxide layer has been calculated at different stages and the results have been verified by the TEM technique. Finally, this study can be useful for investigating the oxide layer thickness and magnetization states of metallic NWs with time grown in polycarbonate templates.

ACKNOWLEDGMENTS

G.H.K. and K.M. acknowledge the WCU (World Class University) program through the National Research Foundation of Korea (NRF) funded by the Ministry of Education, Science and Technology (Grant No. R32-10204). S.K. acknowledges the Pakistan Science Foundation (PSF) for the research Grant No. Phys-145.

[1]V. Franco-Puntes, K. M. Krishnan, and A. P. Alivisatos, Science **291**, 2115 (2001).
[2]A. Hultgren, M. Tanase, C. S. Chen, G. J. Meyer, and D. H. Reich, J. Appl. Phys. **93**, 7554 (2003).
[3]J. Nogués, J. Sort, V. Langlais, V. Skumryev, S. Suriñach, J. S. Muñoz, and M. D. Baró, Phys. Rep. **422**, 65 (2005); C. Diaz-Guerra, M. Vila, and J. Piqueras, Appl. Phys. Lett. **96**, 193105 (2010).
[4]J. Nogués and I. K. Schuller, J. Magn. Magn. Mater. **192**, 203 (1999); M. Fraune, U. Rudiger, G. Guntherodt, S. Cardoso, and P. Freitas, Appl. Phys. Lett. **77**(23), 3815 (2000).
[5]C. Tsang, J. Appl. Phys. **55**, 2226 (1984).
[6]A. Punnoose, H. Magnone, M. S. Seehra, and J. Bonevich, Phys. Rev. B **64**, 174420 (2001).
[7]A. Mumtaz, K. Maaz, B. Janjua, S. K. Hasanain, and M. F. Bertino, J. Magn. Magn. Mater. **313**, 266 (2007).
[8]E. L. Salabas, A. Rumplecker, F. Kleitz, F. Radu, and F. Schüth, Nano Lett. **6**, 2977 (2006).
[9]J. Y. Yu, S. L. Tang, X. K. Zhang, L. Zhai, Y. G. Shi, Y. Deng, and Y. W. Du, Appl. Phys. Lett. **94**, 182506 (2009).
[10]J. C. Salamone, *Polymeric Materials Encyclopedia* (CRC, Boca Raton, 1996).
[11]J. De La Torre Medina, M. Darques, and L. Piraux. J. Appl. Phys. **106**, 023921 (2009).
[12]L. Smardz, U. Kobler, and W. Zinn, J. Appl. Phys. **71**, 5199 (1992).
[13]S. Karim, W. Ensinger, T.W. Cornelius, E. U. Khan, and R. Neumann, J. Nanosci. Nanotech. **8**, 5659 (2008).
[14]W. De Sorbo, Nucl. Tracks **3**, 13 (1979).
[15]K. Maaz, S. Karim, M. Usman, A. Mumtaz, J. Liu, J. L. Duan, and M. Maqbool, Nanoscale Res. Lett. **5**(7), 1111 (2010).
[16]C. Schonenberger, B. M. I. van der Zande, L. G. J. Fokkink, M. Henny, C. Schmid, M. Krueger, A. Bachtold, A. Huber, H. Birk, and U. Staufer, J. Phys. Chem. B **101**, 5497 (1997).
[17]E. Ferain and R. Legras, Nucl. Instrum. Methods Phys. Res. B **174**, 116 (2001).
[18]M. Takahashi, A. Yanai, S. Taguchi, and T. Suzuki, Jpn. J. Appl. Phys. **19**, 1093 (1980).
[19]H. Pan, B. Liu, J. Yi, C. Poh, S. Lim, J. Ding, Y. Feng, C. H. A. Huan, and J. Lin, J. Phys. Chem. B **109**, 3094 (2005).
[20]J. Nogues and I. K. Schuller, J. Magn. Magn. Mater. **192**, 203 (1999).
[21]A. P. Malozemoff, Phys. Rev. B **37**, 7673 (1988).
[22]A. E. Berkowitz and K. Takano, J. Magn. Magn. Mater. **200**, 552 (1999).
[23]K. T.-Y. Kung, L. K. Louie, and G. L. Gorman, J. Appl. Phys. **69**, 5634 (1991).
[24]S. S. P. Parkin and V. S. Speriosu, in *Magnetic Properties of Low-Dimensional Systems II*, edited by L. M. Falicov, F. Mejia-Lira, J. L. Moran-Lopez (Springer, Berlin, 1990), p. 110.
[25]R. Jungblut, R. Coehoorn, M. T. Johnson, J. aan de Stegge, and A. Reinders, J. Appl. Phys. **75**, 6659 (1994).
[26]M. Matsumoto, A. Morisako, S. Takei, and S. Taijima, J. Magn. Soc. Jpn. **21**, 509 (1997).
[27]Y. J. Chen, D. K. Lottis, E. D. Dahlberg, J. N. Kuznia, A. M. Wowchak, and P. I. Cohen, J. Appl. Phys. **69**, 4523 (1991).
[28]Ve. Salgueirino-Maceira, M. A. Correa-Duarte, M. Banobre-Lopez, M. Grzelczak, M. Farle, L. M. Liz-Marzan, and J. Rivas, Adv. Funct. Mater. **18**, 616 (2008).